01 Jan 2023

Finite Line Relief Well System Design for Dams and Levees

Andrew M. Keffer

Erich D. Guy

Katherine R. Grote
Missouri University of Science and Technology, grotekr@mst.edu

Recommended Citation

A. M. Keffer et al., "Finite Line Relief Well System Design for Dams and Levees," *Geotechnical Special Publication*, no. GSP 343, pp. 31 - 48, American Society of Civil Engineers, Jan 2023.
The definitive version is available at https://doi.org/10.1061/9780784484708.004

Finite Line Relief Well System Design for Dams and Levees

Andrew M. Keffer, Ph.D., P.E.[1]; Erich D. Guy, Ph.D., P.G.[2];
and Katherine R. Grote, Ph.D., P.G.[3]

[1]Geotechnical Engineer, US Army Corps of Engineers, Huntington, WV.
Email: Andrew.M.Keffer@usace.army.mil
[2]Chief, Geological Engineering Section, US Army Corps of Engineers, Huntington, WV.
Email: Erich.D.Guy@usace.army.mil
[3]Associate Professor, Geological Engineering, Missouri Univ. of Science and Technology, Rolla, MO. Email: grotekr@mst.edu

ABSTRACT

An analytical method is commonly used to design relief well systems by assuming the well line extends an infinite distance parallel to the dam or levee. This assumption may be met in some cases, but when a well line is of finite length, this can severely underestimate excess heads. Although these consequences have been historically recognized, a practical graph-based analytical approach for finite well line design has not been developed. Finite well lines exist and continue to be installed at many locations, so this study developed a practical design method for such systems. Analytical solutions and numerical models were used to improve understanding of the performance of partial and full penetration finite well systems. Performance was found to be dependent on well system geometry, the ratios of effective seepage entry and exit distances to well spacing, and the number of wells. Model results were used to develop new uplift factors that more accurately define excess heads along and landward of finite well systems that fully or partially penetrate the aquifer.

INTRODUCTION

Relief wells are used by the U.S. Army Corps of Engineers (USACE) and others to safely reduce artesian pressures at the toe of a dam or levee and reduce the risk of internal erosion in the structure's foundation. The existing analytical method in USACE (1992) utilizes closed-form equations to design an infinite line of identical, equally spaced wells to solve for discharge and heads under steady-state confined conditions. There can be detrimental effects of violating the infinite length assumption (USACE 1955, 1963; Bennett and Barron 1957; Guy et al. 2014; Jaeger et al. 2017) wherein excess head would be underestimated. However, development of a practical analytical/chart-based method to design finite well lines is difficult because it must address an array of scenarios and convert complex modeling results into an easily used format.

Key concepts of the differences between infinite and finite systems of various lengths are demonstrated in Fig. 1, which shows plan view finite element (FE) model results for a well line located at the toe of a dam or levee, parallel to seepage entrance and exit boundary conditions. Fig. 1(a) shows a solution for an infinite line of wells, and the head distribution matches what would be calculated using existing analytical solutions. Fig. 1(b, c, d) show the head distribution for finite well lines with differing numbers of wells. When the well line is finite, flow lines are no longer perpendicular to the wells and heads exceed the infinite case. The different head distributions for finite versus infinite lines shown in Fig. 1(a) through 1(d) demonstrate the

potential to underestimate excess head when the infinite design method is used for finite lines. The contour for total head = 25.9 m (85 ft) is shown in each figure to illustrate how the head contours change for different well line designs. The amount of difference depends on parameters in Fig. 1 (e.g. system geometry, number of wells, and boundary distances).

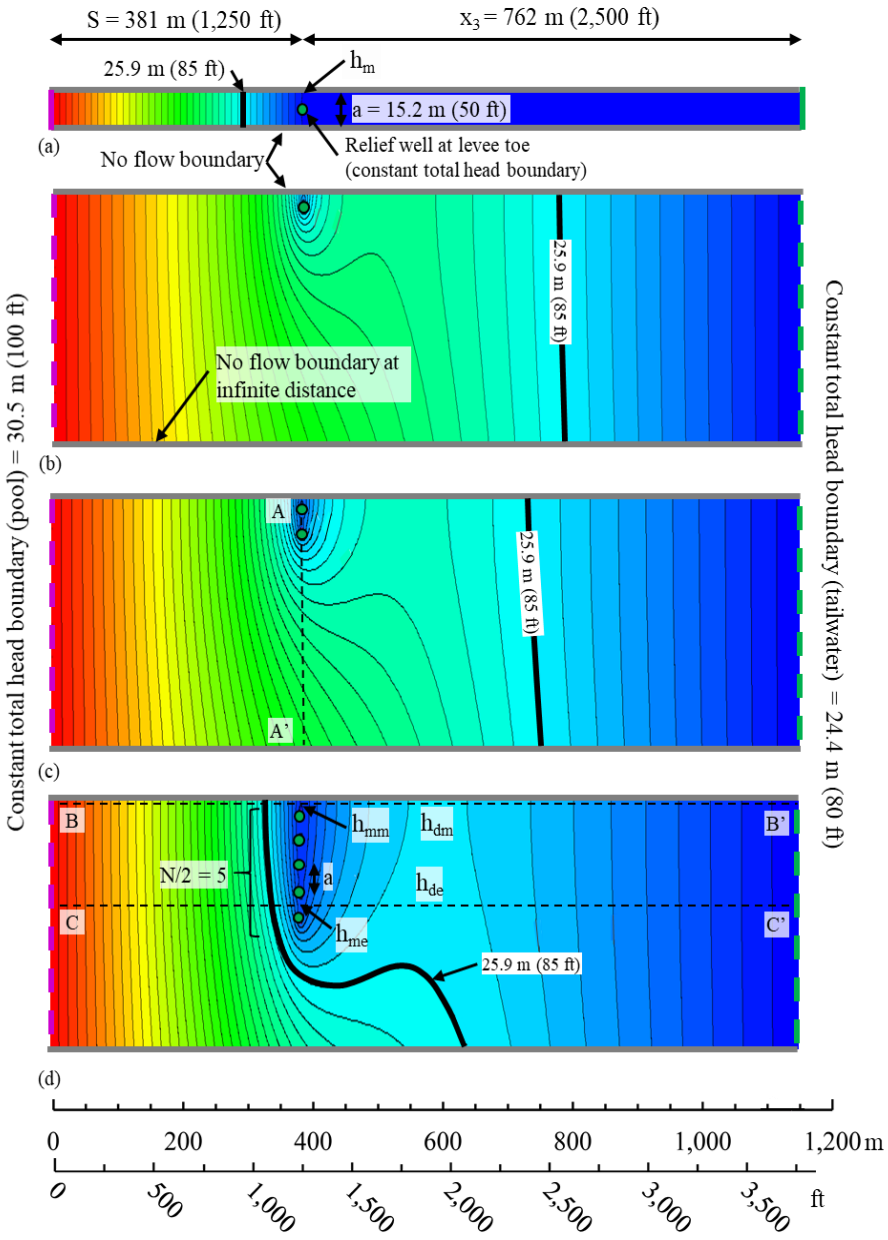

Figure 1. Plan view of head distributions calculated using FE analyses for infinite well lines (a) and finite lines with two (b), four (c), and ten (d) wells. Well locations are shown as green circles, and the head contour interval is 0.15 m (0.5 ft). The 25.9 m (85 ft) total head contour is shown to demonstrate differences in the head distributions. Some key variables are defined here: *S* = distance from effective seepage entrance to landside embankment toe; x_3 = distance from landside embankment toe to effective seepage exit; *a* = well spacing; and *N* = number of wells in a finite line.

Background on infinite versus finite system design methods will introduce the additional complications caused by end-around flow of finite well lines. Performance of infinite and finite relief well systems is studied and contrasted using analytical and numerical models. New design charts were created so that excess head can be estimated along and landward of a finite well line. These charts can be used independently for design, or as a rapid means of verifying FE results.

Infinite Versus Finite Well System Design. Existing methods are based on the Blanket Theory method of underseepage analysis for the base condition (no wells), which was summarized in USACE (1956, 2000, 2018). It computes the midwell excess head (the head half-way between two wells in a well line) (h_m) and average excess head in the well line (h_{av}).

A relief well system is infinite when the wells are equally spaced and identical, the pervious aquifer has uniform depth and hydraulic conductivity, and the infinite seepage entrance and landward exit are parallel to the well line (USACE 1963). Pressure distribution between each well is uniform. However, for a line with finite number of wells (N), head at the middle of the line (h_{mm}) is less than head at the end of that line (h_{me}). A well system can be considered infinite when it is constructed through a long reach of levee or at a dam located within a bedrock valley, and discharge from all wells is equal. Such an impervious boundary is at one-half well spacing ($a/2$) from the end of an infinite system. The lack of such a boundary causes flow that is not perpendicular to the well line and increased, variable pressures. Therefore, the USACE method would calculate h_m or h_{av} and underestimate heads of a finite line. Historically, many sites have experienced issues due to the application of infinite design for finite systems (Guy et al. 2017).

The earliest method to account for well system length relied on graphical construction of a flow net, where the discrete wells were replaced with a line sink (USACE 1952). A single design chart with limited applicability to the middle of a finite well line has been presented in relief well design literature (USACE 1956, 1992; Turnbull and Mansur 1961). Application of this chart is limited by the lack of information it contains regarding input parameters that it can be used for, and it only provides the head at the middle of the well system (not at the end or landward) which is insufficient for design.

A more thorough method was presented in USACE (1963), but also did not include landward heads. However, it requires the use of more than 100 tables with extensive plotting and interpolation, and so is impractical for most engineering applications; no record of its utilization in practice has been found. Keffer and Guy (2021) studied the performance of full penetration finite wells and provided design charts, but that study did not cover partial penetration systems.

INFINITE AND FINITE WELL LINE MODELS

Each well system modeled for this study was first analyzed as an infinite line with the existing analytical method to compute h_m, h_{av}, and discharge from each well (Q_w). A numerical model was run using these same parameters. Agreement between the analytical and numerical modeling results for the infinite system suggest that the model is also appropriate to characterize the finite line systems, where head landward of the wells can be measured.

Infinite Well Line Analytical Model. The existing well design procedure utilizes an adaptation of the Darcy (1856) formula for flow between continuous slots. Distances S and x_3 are illustrated in Fig. 1, and they were introduced in Bennett (1946) and Barron (1948).

The average and midwell uplift factors (θ_{av} and θ_m, respectively) used in relief well design were developed through theoretical and experimental work from the 1930s through the 1950s (USACE 1939a, 1939b, 1949). They account for additional head losses that occur as

groundwater flows along a longer, curved path to a well (rather than the linear path to a slot). They are determined by three dimensionless ratios to account for well system geometry. The ratios are: distance between adjacent wells (a) to well radius (r_w), yielding a/r_w; depth to which the well penetrates (W) into to the total thickness of the homogeneous isotropic pervious foundation (D), yielding W/D; and thickness this foundation to the well spacing, yielding D/a.

The following infinite well line equations are taken from USACE (1992) and shown in corrected form as in Guy et al. (2014). Eq. (1), (2), and (3) compute Q_w, h_{av}, and h_m in terms of net loading on the system (elevation difference between the pool and greater of landside ground surface or ponded tailwater) (h), S, and x_3:

$$Q_w = \frac{k_f \times D \times h}{\frac{S}{a} + \theta_{av}\left(\frac{S+x_3}{x_3}\right)} \tag{1}$$

$$h_{av} = \frac{h \times \theta_{av}}{\frac{S}{a} + \theta_{av}\left(\frac{S+x_3}{x_3}\right)} \tag{2}$$

$$h_m = \frac{h \times \theta_m}{\frac{S}{a} + \theta_{av}\left(\frac{S+x_3}{x_3}\right)} \tag{3}$$

where k_f = effective hydraulic conductivity of the transformed pervious foundation. Eq. (4) computes the net seepage gradient toward the well line (ΔM), which provides another means of calculating discharge and heads of infinite and finite well lines:

$$\Delta M = \frac{h - h_{av}}{S} - \frac{h_{av}}{x_3} \tag{4}$$

Since the study was conducted using the ratio of excess heads for each finite and infinite well system, k_f, D, and h did not affect results as they affected each model equally. The remaining variables that affected results and thus were studied included a/r_w, W/D, D/a, S, and x_3. For finite well lines, the length of the system (L_w) also had to be considered.

A goal of this paper is to provide a practical design tool, so the number of variables in the design tool had to be reduced. Models were normalized for boundary distances and well spacing with the terms S/a and x_3/a. Additionally, θ_{av} and θ_m were used to represent a/r_w, W/D, and D/a. Since L_w (i.e. the distance between the outermost wells) is sensitive to a and the number of wells in a finite line (N) as shown in Eq. (5), finite system length was defined by N (USACE 1963).

$$L_w = a \times (N - 1) \tag{5}$$

Infinite and Finite Well Line Numerical Models. Two- and three-dimensional FE numerical models were used for infinite and finite well systems functioning under steady-state

confined groundwater flow. Fully penetrating wells were modeled in two-dimensional plan view with GeoStudio Seep/W 2020 version 10.2.1.19666 ("GeoStudio" 2020). Partially penetrating wells were modeled in three dimensions with Rocscience RS3 version 4.004 ("Rocscience Inc." 2021). Equal results were obtained for full penetration wells with both programs, but GeoStudio had reduced compute time. Models were constructed similarly in both programs.

A goal of this study was to improve the existing method of design so that it can better handle finite well systems. Results from a FE model can be measured at any location (e.g. landward of the wells), whereas the existing analytical method only reports results along the wells (h_{av} and h_m). These capabilities of the FE models were leveraged to develop advancements to the existing analytical method for infinite well lines.

Fig. 1 illustrates general setup of the models. The pervious foundation with depth D was extended riverward and landward from the wells (perpendicular to the well line axis) to distances of S and x_3, respectively. Well screen geometry was modeled as cylinder elements along the landside levee toe with radius equal to r_w that extended from the top of the foundation to the depth specified by W/D. To model an infinite well line (Fig. 1(a)), foundation width was set equal to a and centered on the well. No-flow boundaries were set perpendicular to the well line located $a/2$ from a single well. These boundaries represent lines of symmetry about which the model could be mirrored. This allows an infinite number of wells to be represented by a single well. Finite well lines were modeled using a similar method; half of each finite line was modeled using an impervious boundary as a line of symmetry perpendicular to and through the middle of the well line. Using a mirrored model produces the same head predictions as were achieved using the full finite well line (length L_w), but the mirrored model reduces compute time. Beginning with the initial infinite line model, one "mirror" impervious boundary was moved very far, on the order of 3,048 m (10,000 ft), from the end (outermost) well, so that an infinite aquifer parallel to the levee was simulated, and head near the end was not influenced.

Steady-state total head boundary conditions were applied to the riverward and landward vertical model faces to represent seepage flow from the loading line source (i.e. pool elevation = 30.5 m (100 ft)) and to the exit line sink (i.e. tailwater, which was equal to ground surface elevation = 24.4 m (80 ft)), respectively. A similar boundary was applied to the relief well to obtain a ground surface (TOG) discharge elevation = 24.4 m (80 ft). These boundaries represent a typical value for net head loading on the levee and well system of h = 6.10 m (20 ft) and are illustrated in Fig. 1. No-flow boundaries were set on the upper (ground surface) and lower (bottom of aquifer) horizontal model faces. The levee was assumed to be impervious (USACE 1992) and exterior boundary conditions were applied at the locations of effective seepage entry and exit, so the embankment geometry was not modeled.

Hydraulic conductivity was set at an isotropic k_f = 0.04 cm/s (100 ft/d) to represent what could be found in a sandy alluvial river valley. A graded tetrahedral mesh was applied to most of each model volume. The graded mesh automatically adjusts element size based on geometric complexity of the model. A uniform mesh with smaller element size was specified in the vicinity of the well line, to a distance of at least a in all directions, so that the curvilinear head contours that develop near the wells were shown accurately. Analytical method results were used to verify the infinite line FE models for excess head and discharge. A comparison of these predicted parameters generated with the FE and analytical models showed a difference of 5% or less.

Key results extracted from finite line models included excess head at the middle of the line (h_{mm}), at the end of the line (h_{me}), maximum head landward of the line's center (h_{dm}), and maximum head landward of the line's end (h_{de}). Measurement locations for these model outputs

are shown in Fig. 1 and 2. These measurements were studied by changing N, S/a, x_3/a, θ_{av}, and θ_m and analyzing results for infinite and finite systems. The overall response of finite line excess heads and how they contrast with infinite line computations will be interpreted and integrated with the existing design method.

RESULTS AND DISCUSSION

The effects of well system length, boundary distances, and system geometry on finite well line results will now be shown and discussed. New charts and equations will be presented to adapt the infinite well line design method to account for finite system length.

Length of Well Line Effects. The scenario illustrated in Fig. 1 was used to demonstrate the effects of N on finite well line performance. For this case, a/r_w = 100, W/D = 100%, and D/a = 1, so θ_{av} = 0.44 and θ_m = 0.55 as determined by USACE (1992). Results are shown in profile view along the well line in Fig. 2, and in profile view normal to the well line in Fig. 3.

These figures demonstrate that head throughout the aquifer were reduced as wells were added to the system. As N increased in Fig. 1, the highlighted head contour (total head = 25.9 m (85 ft)) moved riverward. Fig. 2 shows that h_{mm} approached h_m from the infinite case. Fig. 2(a) displays h_{av} calculated for the infinite line with Eq. (2). Fig. 2(b) plots two ratios: head midway between each well to midwell head of the infinite case ($h_{m\text{-}n}$ / h_m) and discharge from each well to the uniform well discharge of the infinite case ($Q_{w\text{-}n}$ / Q_w) for well lines of various lengths (N = 2 to ∞). While this study focused on providing a design tool to estimate excess heads for a finite well line, Fig. 2(b) gave insight to the non-uniform discharge among the wells. The plot shows that the value of $Q_{w\text{-}n}$ / Q_w at each well fell between the two adjacent values of $h_{m\text{-}n}$ / h_m. So, the flow from a well could be estimated by taking the average of the two adjacent head ratios, and multiplying that by Q_w to obtain $Q_{w\text{-}n}$.

Fig. 3 includes head profiles from the pool to tailwater (perpendicular to the well line) through the middle and end of the well system (sections B-B' and C-C' from Fig. 1). Excess head measurements show the growing difference between head at the center (h_{mm}, h_{dm}) and end (h_{me}, h_{de}) of the finite line as N was increased. The secondary vertical axis in Fig. 3 displays total head so that these head profiles can be visually related to the plan view contours of Fig. 1. For these models, excess head equals the difference between total head and tailwater elevation (which is often assumed equal to the landside ground surface).

Boundary Distance Effects. The scenarios from Fig. 1 (a) and (c) for the infinite case and N = 4 were modified by changing S and x_3 to obtain several values of S/a and x_3/a and to study effects on uplift both along and landward of finite and infinite well lines. Fig. 4 includes model outputs for h_{mm}, h_m, h_{de}, h_{av}, and ΔM (Fig. 4(a) and (b)) and comparison of finite to infinite results through h_{mm} / h_m and h_{de} / h_{av} (Fig. 4(c) and (d)). S/a and x_3/a were varied from 10 to 50.

S/a was held constant while x_3/a was increased for the blue curves in Fig. 4. An increasing x_3/a represents greater confinement of pressures landward of the wells (e.g. thicker or lower conductivity top stratum) that causes more seepage flow to exit the model through the wells. Finite results (h_{mm} and h_{de}) were more affected by x_3 than infinite results. x_3/a was held constant while S/a was increased for the red curves in Fig. 4. An increasing S/a represents less flow down through the riverside top stratum, into the aquifer. This increases the S distance from the well line to the line source loading (i.e. the pool boundary condition). Increasing ratios in Fig. 4(c) and (d) show that finite results were less affected than infinite results.

Fig. 4 illustrates that infinite results (ΔM, h_m, and h_{av}) were more sensitive to S than x_3. This can be explained by Eq. (4) where ΔM is more affected by changes in the first term (contains S)

than the second term (contains x_3) because $(h - h_{av}) > h_{av}$. This sensitivity to S continues through the calculation of h_m and h_{av}, since ΔM affects them (USACE 1992).

Results indicated that h_{mm} / h_m was equally sensitive to each boundary distance (S or x_3) (Fig. 4(c)), but h_{de} / h_{av} in Fig. 4(d) was more sensitive to x_3 than S, as the slope of the line where x_3/a was varied (blue line) was greater than the slope of the line where S/a was varied (red line). Consider two cases in Fig. 4(c) where the opposing values of S/a and x_3/a were reversed. In one case, $S/a = 25$ and $x_3/a = 50$, and for the second case, $S/a = 50$ and $x_3/a = 25$. For both cases, the resulting h_{mm} / h_m were equal. This also occurred for h_{me} / h_m. In Fig. 4(d), this case is represented at the right vertical axis. h_{de} / h_{av} when $x_3 > S$ was greater than when $x_3 < S$. This result probably occurs because h_{de} is landward of the wells; it is more affected by x_3.

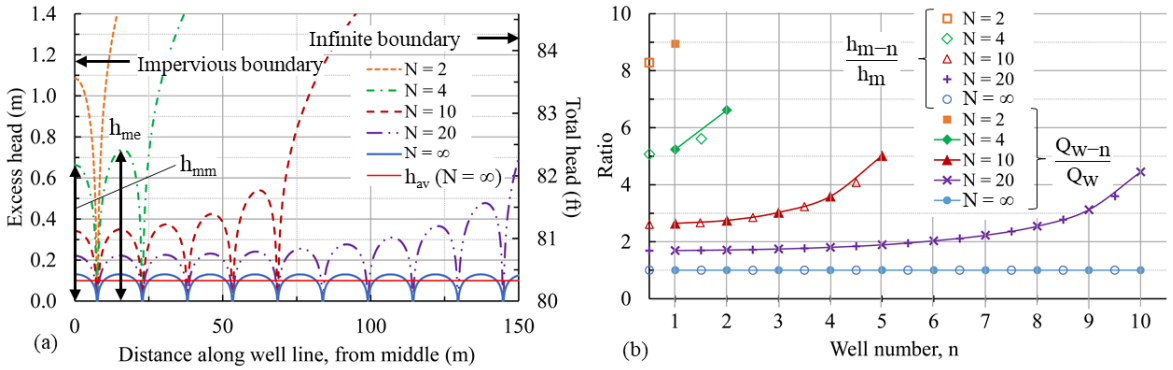

Figure 2. Profile (section A-A' from Fig. 1) of excess head (a) and ratios of finite to infinite results (b) along a well line of various lengths.

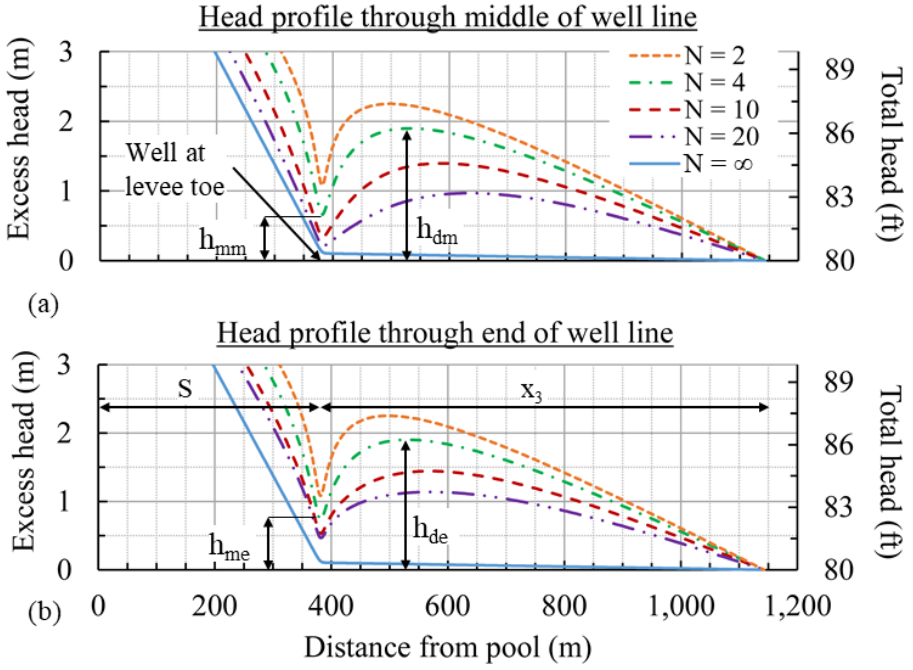

Figure 3. Excess head profile perpendicular to the middle (a) and end (b) of finite well lines of varying lengths (sections B-B' and C-C' from Fig. 1, respectively).

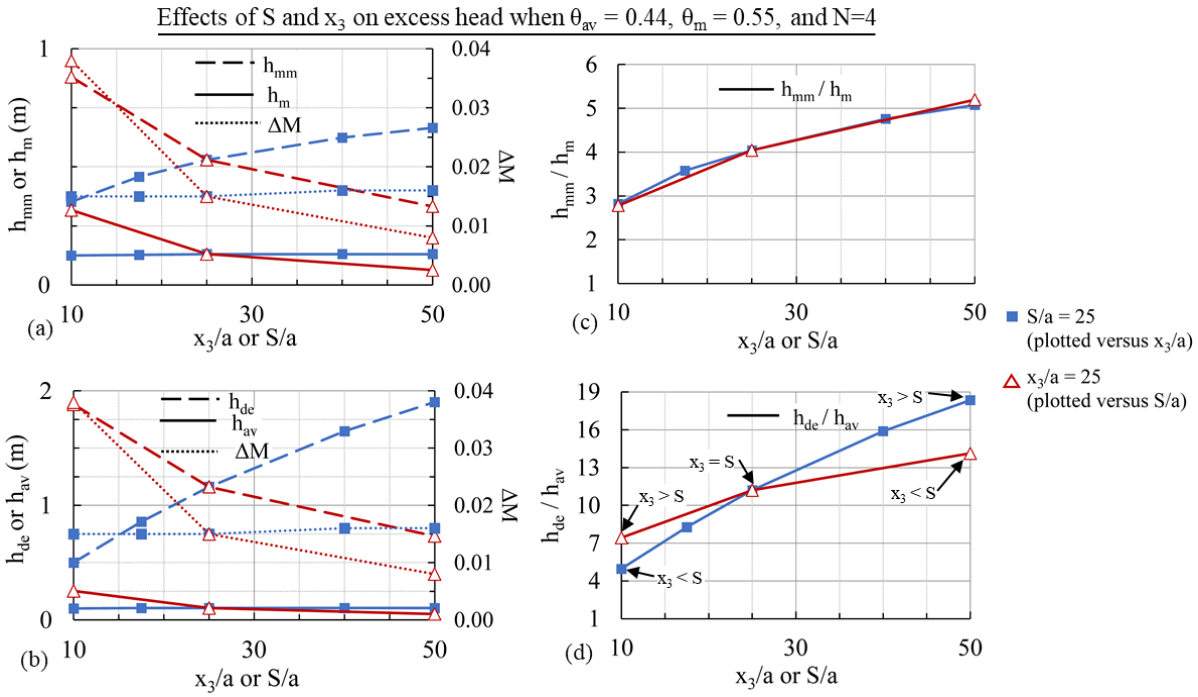

Figure 4. Varying *S* and x_3 plotted against h_{mm}, h_m, h_{de}, h_{av}, and ΔM (a, b) and ratios of finite to infinite line excess heads (c, d).

Well Line Geometry Effects. The geometry of the well system itself was also analyzed for finite line performance. Effects of well system geometry on uplift and discharge in infinite line design are represented by uplift factors θ_{av} and θ_m. θ_{av} and θ_m are determined with input parameters of a/r_w, W/D, and D/a using the existing method. The effects of uplift factors on excess head for finite line systems was investigated by analyzing excess head for each finite line model as the ratio to either h_m or h_{av} (infinite line results). The same value of θ_{av} or θ_m can be obtained for different combinations of a/r_w, W/D, and D/a, but if θ_{av} or θ_m were kept constant (along with other intervening variables N, S/a, and x_3/a), the ratios excess heads for the finite versus infinite well line were consistent. Ratios h_{mm} / h_m and h_{me} / h_m were consistent with each value of θ_m. Infinite line average head (h_{av}) was compared to maximum heads landward of the well line middle and end. Ratios h_{dm} / h_{av} and h_{de} / h_{av} were consistent with each value of θ_{av}.

These ratios were used with θ_{av} and θ_m to create new finite line uplift factors for the middle of line (θ_{mm}), end of line (θ_{me}), landward maximum from the middle of line (θ_{dm}), and landward maximum from the end of line (θ_{de}). θ_{av} and θ_m were multiplied by the relevant head ratio to calculate the respective uplift factors for finite well lines. Scenarios were modeled across the range of θ_{av} and θ_m from USACE (1992), approximately 0.2 to 3.8. Results were used to calculate finite line uplift factors. Fig. 5 shows the general effects of system geometry (e.g. higher a/r_w or lower W/D) that cause uplift resulting from a well system to increase. The infinite and finite uplift factors had a nearly linear relationship in Fig. 5, which will be used in the application of finite line design charts across the range of θ_{av} and θ_m. The new uplift factors will be integrated into new charts and equations for the proposed design method for finite systems.

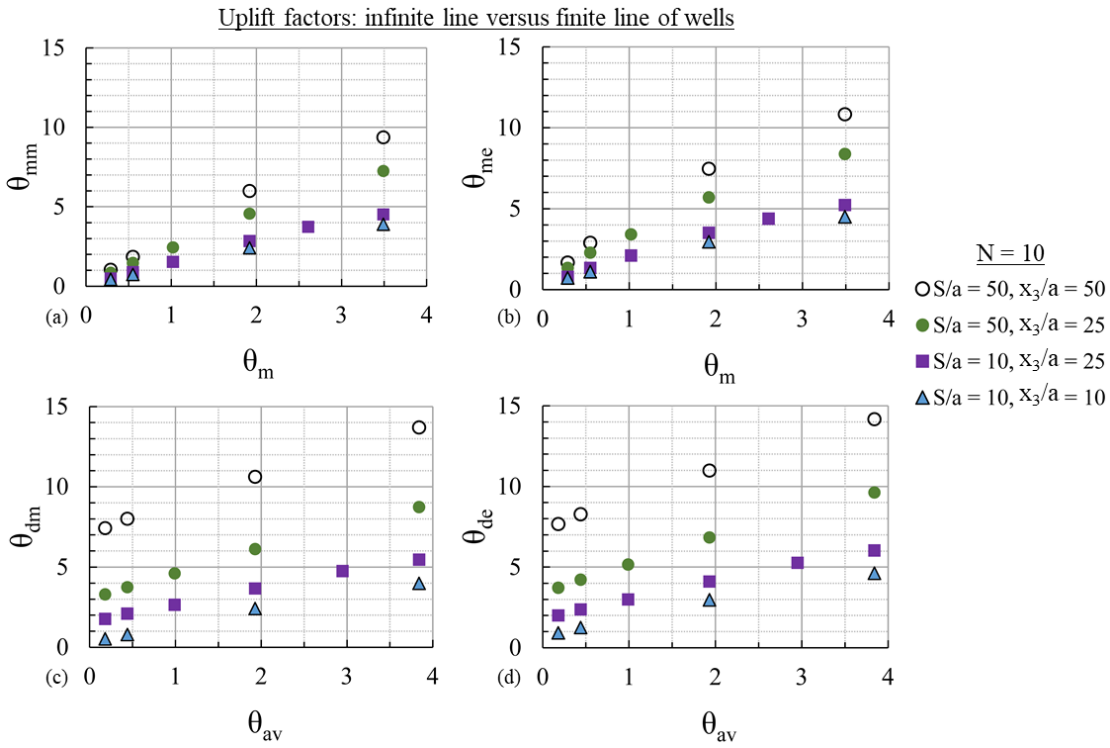

Figure 5. θ_m (a, b) and θ_{av} (c, d) for infinite lines of various geometries plotted against finite line uplift factors for various boundary distances and N = 10.

Design Method for Finite Well Lines. As shown by Fig. 1 through 5, excess heads may be severely underestimated if a finite line of wells is analyzed as infinite, so accounting for *N* is important. FE models were used to understand relationships among finite line performance and the number of wells, distance to pool and tailwater boundaries, and the system geometry, and build charts and equations that adapt the existing infinite method to account for finite systems.

Finite line uplift factors were defined across the ranges of infinite line θ_{av} and θ_m from the existing method. For in-line uplift factors (θ_{mm} and θ_{me}), θ_m = 0.29; 1.92; and 3.49 are included in new design charts (Fig. 6 and 7). For landward uplift factors (θ_{dm} and θ_{de}), θ_{av} =0.18; 1.93; and 3.84 are included (Fig. 8 and 9). It is not practical to present data for every value of θ_m and θ_{av}, so this approach allows interpolation by presenting design charts for lower, midrange, and upper values. Results include *N* from 2 to 20 and various combinations of *S/a* and x_3/a which each ranged from 5 to 50. Some combinations of *S/a* and x_3/a are not included on Fig. 6 through 9 to aid legibility, but they are not critical to the charts' function, as omitted curves would be intermediate values within a relatively small range of finite uplift factors. Fig. 6 through 9 can be used for scenarios with parameters that would fall between the plotted values of *S/a*, x_3/a, θ_{av}, or θ_m via linear interpolation as demonstrated by Fig. 4 and 5.

For most of the curves in Fig. 8 and 9, θ_{dm} and θ_{de} are greater than θ_{av}. But for some cases with $N > 4$, θ_{dm} or θ_{de} approach an infinite-acting state and are less than θ_{av}. This occurs because the average head has been used as a conservative estimation of infinite line landward head (USACE 1955). Curves in Fig. 8 and 9 also tend to cross each other more than those in Fig. 6 and 7 because the θ_{dm} and θ_{de} are more sensitive to x_3/a than *S/a* (Fig. 4).

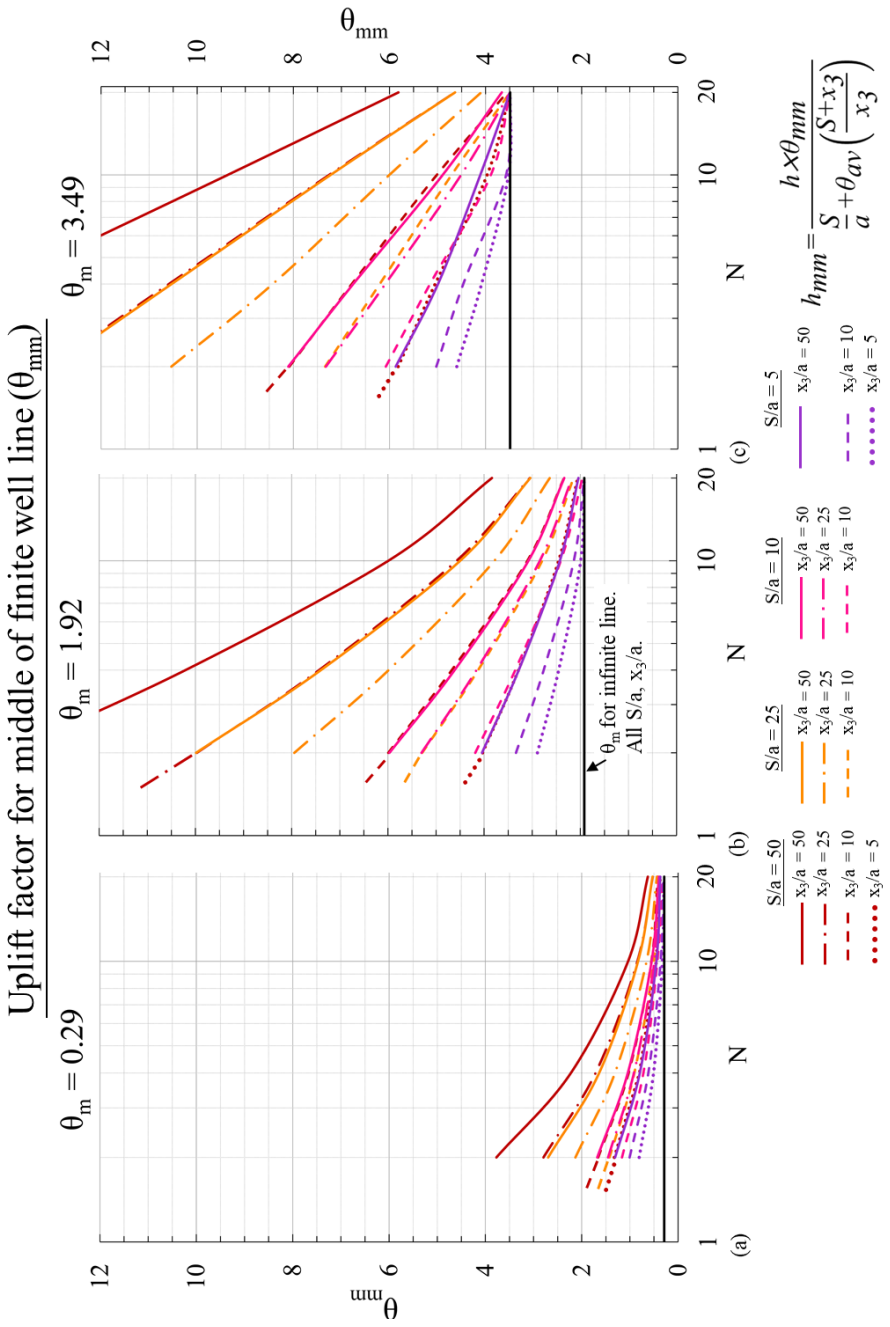

Figure 6. θ_{mm} for finite well lines for infinite lines with θ_m = 0.29 (a), 1.92 (b), and 3.49 (c).

Head results for well systems at dams or levees are typically analyzed and evaluated based on a desired effective stress uplift factor of safety (*FS*), based on the buoyant unit weight and thickness of the top stratum (Duncan et al. 2011; Guy et al. 2014; Sills and Vroman 2007), to achieve an acceptable head value (h_a) at the base of a confining top stratum. *FS* is calculated by:

$$FS = \frac{\gamma_{b\text{-}bl} \times z_{bl}}{\gamma_w \times h_{excess}} \tag{6}$$

where $\gamma_{b\text{-}bl}$ = buoyant unit weight of landside top stratum; γ_w = unit weight of water; z_{bl} = thickness of landside top stratum; and h_{excess} = maximum computed excess head. If *FS* in Eq. (6) is set equal to the desired minimum, then h_{excess} can be calculated to determine h_a.

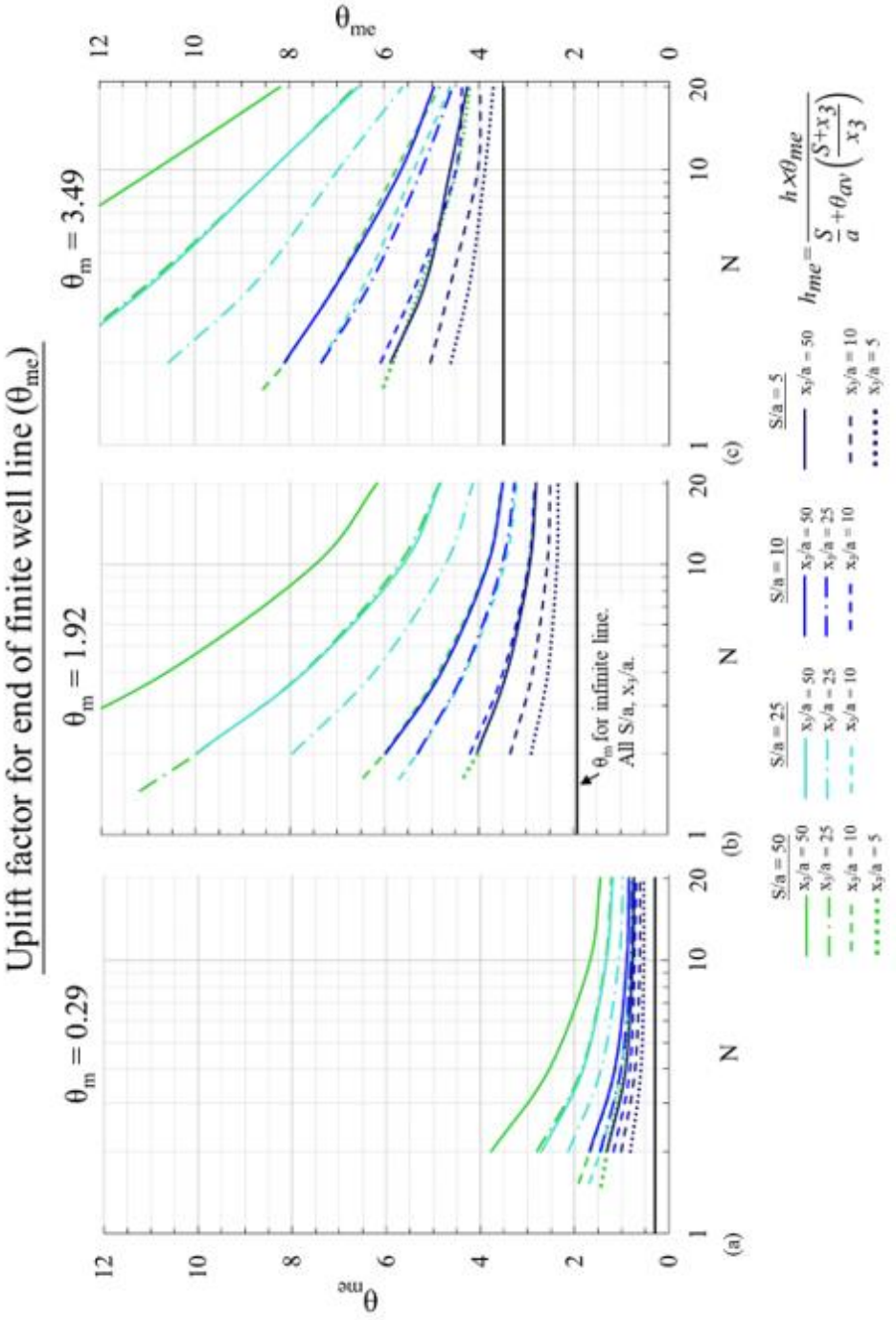

Figure 7. θ_{me} for finite well lines for infinite lines with θ_m = 0.29 (a), 1.92 (b), and 3.49 (c).

After applying the infinite method to find θ_{av} and θ_m (based on a/r_w, W/D, and D/a), Fig. 6 through 9 can incorporate the number of wells in the finite line and determine θ_{mm}, θ_{me}, θ_{dm}, and

θ_{de}. The new uplift factors are then used to calculate h_{mm}, h_{me}, h_{dm}, and h_{de} to characterize uplift along and landward of the finite well system with Eq. (7), which is modified from infinite line Eq. (2) and includes the USACE (1992) approach based on ΔM:

$$h_{XX}=\frac{h\times\theta_{XX}}{\frac{S}{a}+\theta_{av}\left(\frac{S+x_3}{x_3}\right)}=(a)(\Delta M)(\theta_{XX}) \tag{7}$$

Substitute θ_{XX} in Eq. (7) with each finite uplift factor (substitution is shown in Fig. 6 through 9) to calculate excess head values for h_{XX}. These can be used for h_{excess} in Eq. (6) to calculate *FS*.

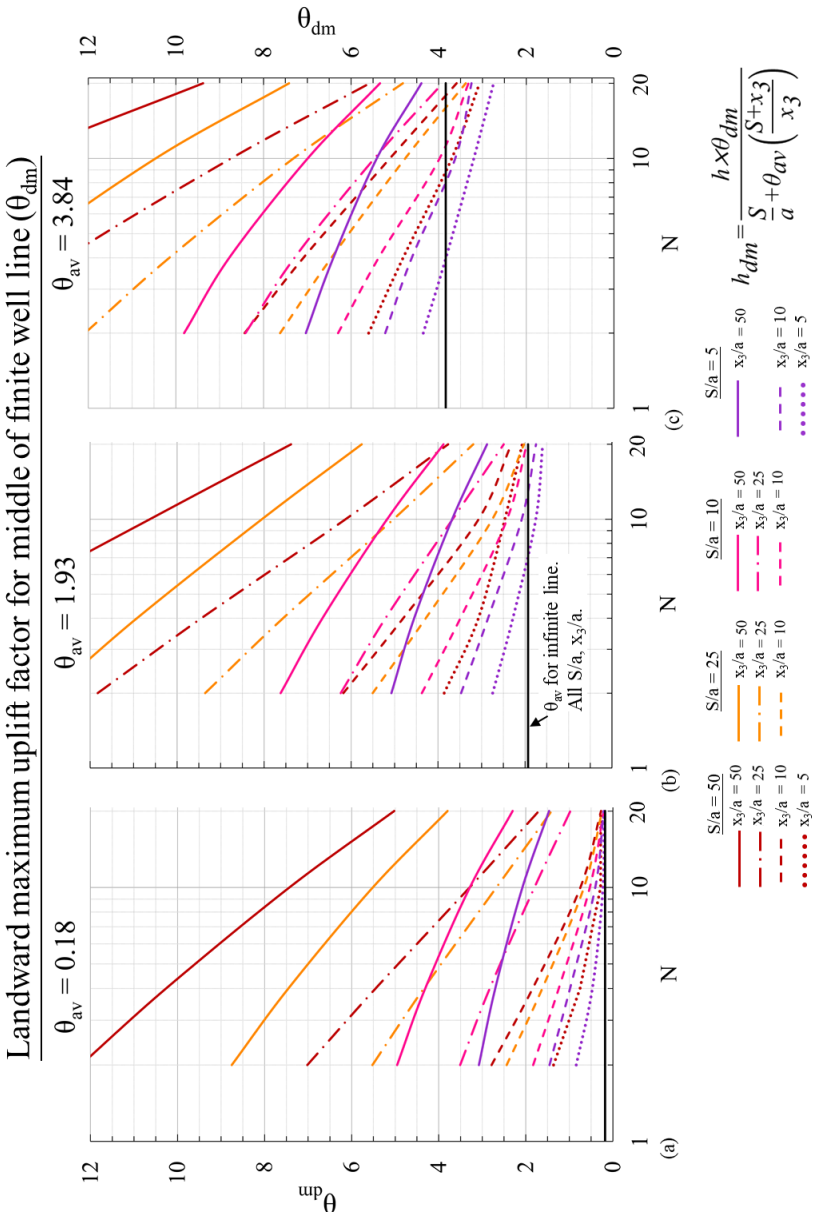

Figure 8. θ_{dm} for finite well lines for infinite lines with θ_{av} = 0.18 (a), 1.93 (b), and 3.84 (c).

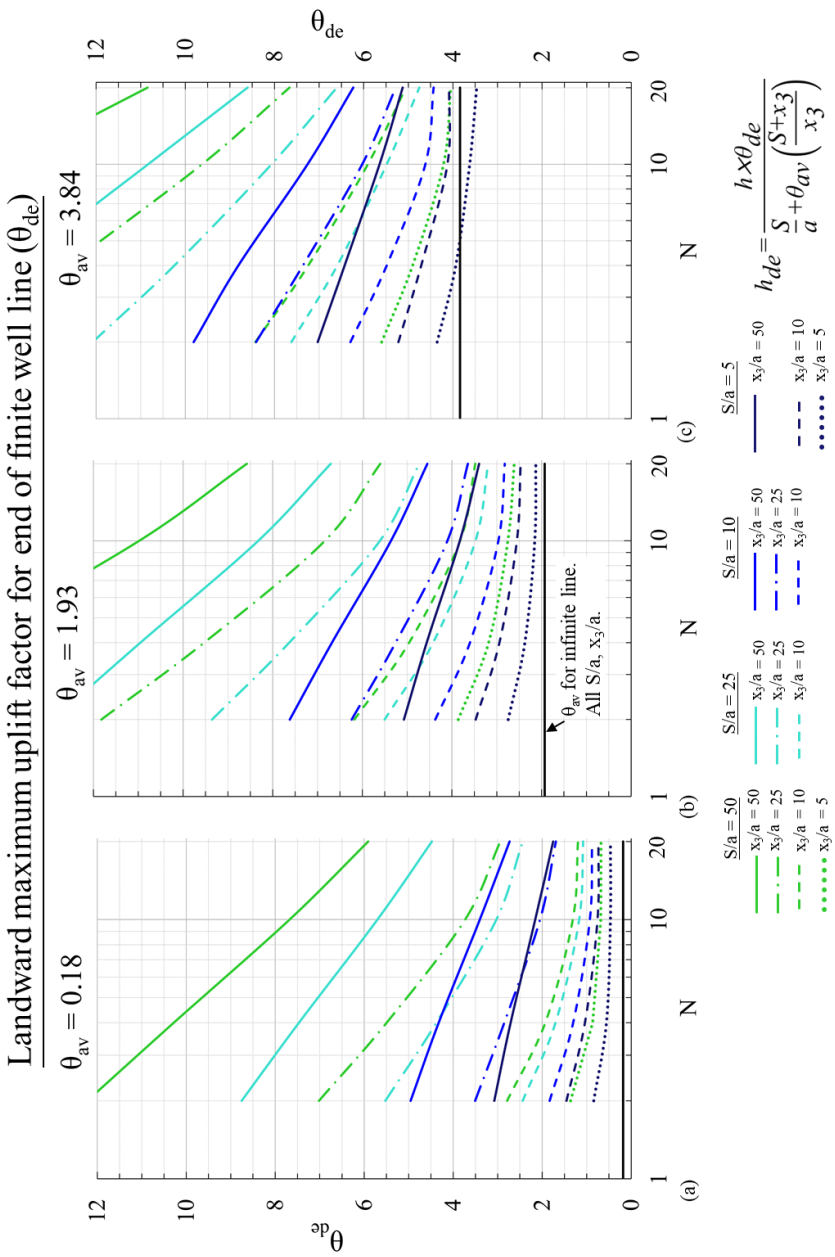

Figure 9. θ_{de} for finite well lines for infinite lines with θ_{av} = 0.18 (a), 1.93 (b), and 3.84 (c).

The designer must consider site conditions and objectives to determine the location(s) at which uplift should be evaluated by *FS*. A pumping station is an example of an isolated location with problematic underseepage. In this case, a finite well line may be designed with its center located at the pumping station, so only θ_{mm} and θ_{dm} (and therefore h_{mm} and h_{dm}) need to be calculated. The application of the new charts and equations to will now be demonstrated.

FINITE WELL LINE DESIGN EXAMPLE

An example reach of levee includes a pumping station (which discharges stormwater from the area protected by the levee) where underseepage countermeasures need to be designed, so a

relief well system will be analyzed to demonstrate the use of the new design charts in Fig. 6 through 9. Key geologic and loading parameters were defined in Table 1. h, S, and x_3 were used to calculate base condition excess head as h_o = 4.93 m (16.2 ft) with USACE (2000). Eq. (6) was used to calculate FS = 0.5 for the base condition (no wells, so $h_o = h_{excess}$), which was unacceptable. In this case, excess head is defined as the difference between a piezometer reading at the top of the aquifer and the top of ground. For this problem a design FS = 2 was selected and used to calculate $h_{excess} = h_a$ = 1.28 m (4.21 ft) as an acceptable value that should be targeted by the well system design along the levee toe. For locations farther landward of the levee, a minimum acceptable FS = 1.5 was selected and a landward value of h_a = 1.71 m (5.62 ft) was calculated. These values of h_a that are in Table 1 apply to the low area at the pump station because this is where the lowest value of z_{bl} exists. h_a would be larger, nearly double, elsewhere along the levee (at locations of h_{me} and h_{de}) because z_{bl} increases away from the pump station. The ponding area could be visualized as a depression in the ground surface landward of the well line to the tailwater boundary which is 7.62 m (25 ft) wide measured along the levee.

Table 1. Loading and geologic parameters for the example problem.

Parameter	Value	Parameter	Value
Pool	133.50 m (438 ft)	S	274.0 m (899 ft)
TW=TOG	124.97 m (410 ft)	x_3	375.2 m (1,231 ft)
Top of well elev.	124.97 m (410 ft)	h_o	4.93 m (16.2 ft)
h	8.53 m (28 ft)	Base FS	0.5
z_{bl}	3.05 m (10 ft)	Design in-line FS	2.0
$\gamma_{b\text{-}bl}$	8.27 kN/m^3 (52.6 lb/ft^3)	Design landward FS	1.5
k_f	1.83x10^{-2} cm/s (52 ft/d)	In-line h_a	1.28 m (4.21 ft)
D	114.3 m (375 ft)	Landward h_a	1.71 m (5.62 ft)

This example assumes there are no hydraulic- or elevation-related well losses. Hydraulic (friction and velocity within the filter pack, screen, and riser) losses are not linear with flow and are specific to each site and well system (Bennett and Barron 1957), so they could not be incorporated into the new design charts. Head losses should be considered in practice. Losses can be estimated via pumping tests at the design discharge or with USACE (1992).

Consider a finite system with W/D = 50%, a = 35.05 m (115 ft), and N = 10 wells as listed in Table 2. Eq. (2) and (3) were used to calculate h_{av} and h_m (h_{av} is greater and would govern this infinite line design), which are lower than the values of h_a in Table 1, but don't account for line length. The spreadsheet program in Guy et al. (2010) performs computations in agreement with USACE (1992) and was used to perform the infinite line analyses. Infinite line computations for θ_{av}, θ_m, h_{av}, and h_m are included in Table 2. For finite line computations, values of θ_{av}, N, S/a, and x_3/a were used in Fig. 6 through 9 design charts to determine θ_{mm}, θ_{me}, θ_{dm}, and θ_{de}. Since θ_m and θ_{av} in Table 2 are not the same as values included in the new design charts (they rarely will be the same; this method will often involve interpolation), the two charts on either side of each value

will be used. Since the values are between parts (a) and (b) from each chart in Fig. 6 through 9, parts (a) and (b) were each read for finite uplift factors. These results are included in Table 3 and were interpolated between to the desired infinite and finite uplift factors in Table 2 (via the linear forecast function in Microsoft Excel). In these interpolations, infinite line θ_m or θ_{av} are the independent variables and finite line θ_{mm}, θ_{me}, θ_{dm}, or θ_{de} are the dependent variables. θ_{mm}, θ_{me}, θ_{dm}, and θ_{de} were used in Eq. (7) to calculate h_{mm}, h_{me}, h_{dm}, and h_{de} listed in Table 2 for the finite line. Table 2 values of h_{mm} and h_{dm} are lower than their respective values of h_a specified in Table 1, so this design meets the uplift safety factor criteria at and landward of the well line. Excess head at and landward of the line's end (h_{me}, h_{de}) exceed the acceptable values in Table 1. This is allowable because, in this example, uplift resistance increases beyond the end of the well line. A finite line FE model resulted in excess heads within 5% of the chart solutions.

Table 2. Input parameters and results for trial well system in example problem to achieve acceptable *FS*. θ_{mm}, θ_{me}, θ_{dm}, θ_{de} were computed by interpolating between values in Table 3.

Parameter	Infinite line	Finite line	Parameter	Infinite line	Finite line
a	35.05 m (115 ft)	35.05 m (115 ft)	N	-	10
a/r_w	115	115	L_w	-	315.5 m (1,035 ft)
D/a	3.3	3.3	θ_{mm}	-	1.29
W/D	50%	50%	θ_{me}	-	1.63
θ_{av}	1.45	-	θ_{dm}	-	1.70
θ_m	1.07	-	θ_{de}	-	2.21
S/a	7.8	7.8	h_{mm}	-	1.07 m (3.50 ft)
x_3/a	10.7	10.7	h_{me}	-	1.35 m (4.42 ft)
ΔM	0.0236	-	h_{dm}	-	1.41 m (4.61 ft)
Q_w	1,497.2 m^3/d (274.7 gpm)	-	h_{de}	-	1.83 m (5.99 ft)
h_{av}	1.20 m (3.93 ft)	-			
h_m	0.88 m (2.90 ft)	-			

For the example problem finite line in Table 2, central well discharge would be estimated as 1,497.2 m^3/d x (1.07 m / 0.88 m) = 1,820.5 m^3/d (334.0 gpm). Outermost well discharge would be estimated as 1,497.2 m^3/d x (1.35 m / 0.88 m) x 120% = 2,756.2 m^3/d (505.6 gpm). The 120% is included because h_{me} is between the outermost two wells and therefore h_{me} / h_m will underestimate the actual outer well discharge typically by 20% when compared to model results. Taking the average of these two values and N = 10, total system flow would be estimated as 2,288.4 m^3/d x 10 = 22,884 m^3/d (4,198 gpm). Total system flows estimated by this approach were found to agree with FE modeling results, having less than a 2% difference for the same problem. This demonstrates that well discharges in a finite line exceed that of a single well in an otherwise identical infinite line, which for this problem is Q_w = 1,497.2 m^3/d (274.7 gpm). Well discharges in a finite line are greater because with fewer wells there is greater head along the line to drive flows.

S/a and x_3/a often will not match the curves in Fig. 6 through 9. For example, *S/a* = 7.8 and x_3/a = 10.7 in Table 2, but *S/a* or x_3/a = 5; 10; 25; and 50 in Fig. 6 through 9. Users can solve for other values of *S/a* or x_3/a with visual estimation or linear interpolation with readings from each curve for the needed value of *N*. This approach was used to find uplift factors reported in Table 3 for the example *S/a* and x_3/a.

Table 3. Chart results for θ_{mm} and θ_{me} (Fig. 6 and 7) and θ_{dm} and θ_{de} (Fig. 8 and 9) when *S/a* = 7.8; x_3/a = 10.7; and *N* = 10. Interpolation between these uplift factors was used to compute results for θ_m = 1.07 and θ_{av} = 1.45 for infinite line and finite line in Table 2.

Parameter	Fig. 6a, 7a	Interpolated	Fig. 6b, 7b	Fig. 8a, 9a	Interpolated	Fig. 8b, 9b
θ_{av}	-	-	-	0.18	1.45	1.93
θ_m	0.29	1.07	1.92	-	-	-
θ_{mm}	0.40	1.29	2.25	-	-	-
θ_{me}	0.70	1.63	2.65	-	-	-
θ_{dm}	-	-	-	0.50	1.70	2.15
θ_{de}	-	-	-	0.90	2.21	2.70

SUMMARY AND CONCLUSIONS

Relief well systems are regularly employed for underseepage control at dams and levees, often in the form of a finite line. If the infinite line method is used to determine well spacing for a finite line, the result would likely be an incorrect system design where excess head is not reduced to an acceptable level. To date, there has been neither a practical graph-based means to analyze these problems nor to verify solutions from other methods. This has been due to the challenge of reducing and evaluating data from the numerous models needed to represent the range of potential design scenarios. In this study, parameters affecting finite solutions were identified, and intervening variables were utilized to develop such an approach for determining in-line and landward heads across the general range of practical design parameters. Numerical models were used to characterize finite line performance when the number of wells, distance to boundary conditions, and system geometry were varied. Head along the finite line and the landward maximum were found to be related to the midwell and average heads of the infinite line, respectively. The new design process developed for a finite line of relief wells was illustrated with an example problem. Given the complexity of finite well line behavior, this study provided further understanding of the topic and a process which can be used for design or verification.

ACKNOWLEDGMENTS

The authors thank Dr. Michael Navin and Noah Vroman from the USACE Levee Safety Center and Patrick Conroy, retired from USACE, for their overall advancement of Blanket Theory and relief wells practice and for their support of and contributions to this study.

REFERENCES

Barron, R. A. (1948). "The Effect of a Slightly Pervious Top Blanket on the Performance of Relief Wells." In *Proc., 2nd Int. Conf. Soil Mech. and Found. Eng.*, Vol. 4, ISSMGE, p. 324-328.

Bennett, P. T. (1946). "The Effect of Blankets on Seepage through Pervious Foundations." *ASCE Transactions*, 111 (1), p. 215-228.

Bennett, P. T., and Barron, R. A. (1957). "Design Data for Partially Penetrating Relief Wells." In *Proc., 4th Int. Conf. on Soil Mech. and Found. Eng.*, Vol. 2, Div. 3b-6, p. 282-285. London.

Darcy, H. (1856). *The Public Fountains of the City of Dijon*. Paris (in French).

Duncan, J. M., O'Neil, B., Brandon, T., and VandenBerge, D. R. (2011). "Evaluation of Potential for Erosion in Levees and Levee Foundations." Center for Geotechnical Practice and Research #64, Virginia Tech, 36 p.

GeoStudio. (2020). Geoslope.com. https://www.geoslope.com/products/seep-w.

Guy, E. D., Nettles, R. I., Davis, J. R., Carter, S. C., and Newberry, L. A. (2010). "Relief Well System Design Approach: HHD Case Study." In *Association of State Dam Safety Officials Proceedings*, Charleston, WV, 19 p.

Guy, E. D., Ider, H. M., and Darko-Kagya, K. (2014). "Several Relief Well Design Considerations for Dams and Levees." In *Proceedings of the 45th Annual Ohio River Valley Soils Seminar*, Cincinnati, OH, p. 81-106.

Guy, E. D., Darko-Kagya, K., Spagna, S. S., and Keffer, A. M. (2017). "Portsmouth Levee Foundation Erosion Incident." In *Association of State Dam Safety Officials Southeast Regional Conference Proceedings*, Nashville, TN, 8 p.

Jaeger, R. A., Keizer, R. A., Bradner, G. C., Weber, J. P., and Stanley, M. H. (2017). "Advances in Design Procedures for Relief Well Lines in Variable Urban Settings." In *USSD (United States Society on Dams) Annual Conference Proceedings*, Anaheim, CA, 20 p.

Keffer, A. M., and Guy, E. D. (2021). "Design Method for a Finite Line of Fully Penetrating Relief Wells." In *Proc., 10th International Conference on Scour and Erosion (ICSE-10)*, Online, 18-21 October 2021, p. 1284-1298.

Rocscience Inc. (2021). Rocscience Inc. https://www.rocscience.com/software/rs3.

Sills, G. L., and Vroman, N. (2007). "A Review of Corps of Engineers Levee Seepage Practices in the United States." In *Internal Erosion of Dams and their Foundations*, London: Taylor & Francis Group, p. 209-218.

Turnbull, W. J., and Mansur, C. I. (1961). "Design of Control Measures for Dams and Levees." *ASCE Transactions*, 126 (1), p. 1486-1522.

USACE. (1939a). *Mississippi River Levees Underseepage Studies – Black Bayou Levee*.

USACE. (1939b). "The Efficacy of Systems of Drainage Wells for the Relief of Subsurface Hydrostatic Pressures." Technical Memorandum TM 151-1, Waterways Experiment Station, Vicksburg, MS.

USACE. (1949). "Relief Well Systems for Dams and Levees on Pervious Foundations, Model Investigations." Technical Memorandum TM 3-304, Waterways Experiment Station, Vicksburg, MS.

USACE. (1952). "Control of Underseepage by Relief Wells, Trotters, Mississippi." Technical Memorandum TM 3-341, USACE Mississippi River Commission, Waterways Experiment Station, Vicksburg, MS.

USACE. (1955). "Relief Well Design." Civil Works Engineer Bulletin 55-11, Washington, DC.

USACE. (1956). “Investigation of Underseepage and its Control, Lower Mississippi River Levees.” Technical Memorandum TM 3-424, USACE Mississippi River Commission, Waterways Experiment Station, Vicksburg, MS.
USACE. (1963). “Design of Finite Relief Well Systems.” Engineer Manual EM 1110-2-1905, Washington, DC.
USACE. (1992). “Design, Construction, and Maintenance of Relief Wells.” Engineer Manual EM 1110-2-1914, Washington, DC.
USACE. (2000). “Design and Construction of Levees.” Engineer Manual 1110-2-1913, Washington, DC.
USACE. (2018). “Comparison of Levee Underseepage Analysis Methods Using Blanket Theory and Finite Element Analysis.” Engineer Research and Development Center, Geotechnical and Structures Lab. Tech. Report TR-18-14. 145 p.